Are Spiral Galaxies Round?

Richard McDonald
June 10, 2006

Introduction

This project began as an exploration of the use of observational measurement and statistical techniques to test the hypothesis H_0 that *all spiral galaxies are perfectly round and that the elliptical shapes we see correspond to the projection effect of our viewing angle on their randomly-inclined disks*. As I discovered that I lack the measurement precision and the mathematical tools to make an accurate analysis of this hypothesis, the project expanded into a sample of these techniques, analysis of catalogue data, simulation of a theoretical case, and a survey of recent research on this and related questions.

My results are mixed. I was able to answer the posed question, "are spiral galaxies round?" as "generally yes, within my available precision" with some confidence, based on visual analysis of distribution graphs. I was unable, however, to fit the theoretical distribution to observations with statistical techniques.

Modern research is determining that spiral galaxies are not, in fact, round, but have a slight ellipticity. I show where some minor anomalies in my data may be attributed to this ellipticity. However, I was unable to reproduce the data analysis that is leading researchers to these conclusions. My attempt to compare the ellipticity theory to observed data by using a simulation was visually suggestive, but also failed statistical significance tests.

Measuring Method

Calculating Apparent Inclinations

Observing a collection of galaxies at random locations in the sky, one observes a variety of ellipses of varying eccentricity, and rotated at varying angles from horizontal, as illustrated in Figure 1. I make the simplifying assumption that the angle of rotation from horizontal can be ignored, since it does not affect observed ellipticity, as do rotations in the other 2 dimensions (Rood and Baum 1967), so only the lengths of the perpendicular major and minor axes of the ellipses are recorded.

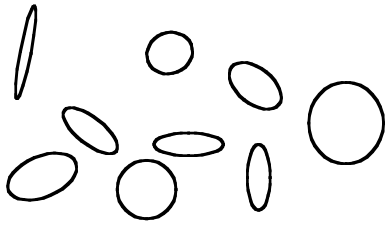

Figure 1: Random Ellipses

In fact, recent findings indicate this assumption is untrue – position angles of galaxies are not random, but are oriented so that the galaxies are aligned with the filaments in recently-discovered large-scale structure (Trujillo, Carretero et al. 2006). However, this effect is too small for detection in a study such as this project, and can safely be ignored.

We can also ignore inclinations greater than 90° since larger inclinations would simply present other faces of the galactic disk but would still project as ellipses.

Basic conical-section geometry shows that a circle inclined away from the viewer by an angle θ (where $\theta = 0$ is face-on) will project as an ellipse where the ratio of the minor to major axes is

$$b/a = \cos\theta$$

Equation 1

(Eshbach 1936). Figure 2 shows the inclination of a circle producing an ellipse. This circle is theoretical, with zero thickness.

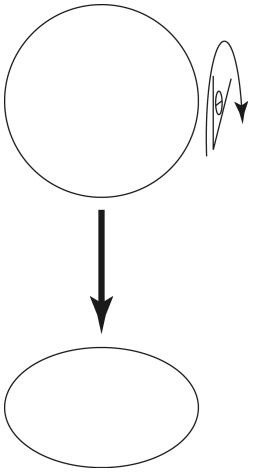

Figure 2: Inclined Circle becomes Ellipse

Real galaxies, on the other hand, have a non-zero thickness. They would be best modelled by two concentric ellipsoids, one for the bulge and one for the disk, but can be closely approximated by an ellipsoid with a thickness of 10% to 20% of the disk diameter (Sandage, Freeman et al. 1970) The intrinsic thickness of a galaxy limits the thinness that can be observed when the galaxy is viewed edge-on. For example, Figure 3 (page 14) shows an ellipsoid galaxy (a=10, b=9, c=2) viewed from above, showing only a normal projection ellipse. When viewed directly edge-on, however, Figure 4 shows the thinnest observable ellipse, corresponding to the thickness of the galactic disk.

Hubble (1926) derived a formula for translating the observed axis ratio to inclination angle for a disk as

$$\cos^2\theta = \frac{(b/a)^2 - q_0^2}{1 - q_0^2}$$

Equation 2

where q_0 is the "inherent thickness", or the c-axis, of the ellipsoid. It was common in early analyses to use a fixed value such as 0.20 for q_0 (Tully 1972), (Tully and Fisher 1977). More recently, the thickness correction has been found to vary with the galaxy's morphological type (Ryden 2005). I found the q_0 tables of Haynes (1984) and Nedyalkov (1993), as shown in Figure 5 (pg. 15), improved the fit of highly-inclined galaxies significantly. Finally, Aaronson et al (1980) recommend adding a fixed 3° correction to account for "systematic differences between RC2 ratios and radio observations". I experiment with this correction in the analysis below.

Expected Distribution

Before analyzing available data, I considered what kind of distribution I would expect to find if H_0 were true.

Clearly, if I truly were observing an unbiased random sample of randomly-inclined disks, and if all the ellipses observed were disks rotated on a single axis of rotation, I would expect a uniform distribution of my calculated inclination angles (Huizinga and Albada 1992). Figure 6 shows such a distribution from an artificially-generated sample.

However, although I am *modelling* the ellipses as disks with a single rotation, they are in *reality* disks rotated on two axes. (In fact, *three*, but I am ignoring position angle.) That is, if we assume the disk started face-on to us, we then have to rotate it on the "horizontal" axis, and then on the "vertical" axis to achieve any possible orientation in space. This second rotation will drive the distribution we see away from a uniform distribution. Since the ratio of the two axis lengths is related to the second rotation by $b/a = \cos\theta$ and therefore $\theta = \arccos(b/a)$, I would expect to see calculated inclinations distributed as arccosine. (I confess that I had to visually inspect the measured distributions of my catalogue samples, hunting for an explanation of the sine-shaped hump before realizing what was happening. The fact that many curves exhibited a peak near 60°, which is cos(1/2), was a clue.) Figure 7 (pg. 16) shows the distribution of inclinations calculated from artificially-generated a and b axis lengths. This strongly resembles an arccosine probability density, as seen by comparing to a theoretical arccosine density shown in Figure 8.

Interestingly, this distribution suggests that face-on galaxies should be rarely observed. This is intuitive, since there are two dimensions of rotation that can take a galaxy away from a face-on view, and only identical rotations in both of those dimensions leaves it appearing to face the observer. One would expect this to be a low-probability occurrence. Also, the central tendency (here peaking at 70-80 degrees) might shift left or right depending on the optical depth of the galaxies. If galaxies were largely opaque, then edge-on galaxies would be underrepresented in a large sample (Disney 1990) – contrary

to the relatively high representation of edge-on galaxies the arccosine distribution predicts.

Data Collection

Both for my own measurements and, later, for catalogue analysis, I followed the lead of many researchers who select spiral galaxies with certain properties. I preferred Hubble types Sa and later for their distinct disk shapes (Tully and Fisher 1977), avoided Barred spirals because Bars can distort dimension measurements, especially in visible wavelengths (Ryden 2004), selected disks with a large apparent diameter for easy measurement (Binney and de Vaucouleurs 1981), and manually rejected images that showed obvious signs of interaction or distortion (Nedyalkov 1993).

For my own measurements, I downloaded images from the Internet, most from the Digital Sky Survey (Erdmann undated). I inspected these images in negative using Adobe Photoshop. Assuming that position angle is irrelevant, I rotated each image to bring the galaxy's major axis horizontal, and then used the Photoshop ellipse tool to visually fit an ellipse over the galaxy, measuring the dimensions in pixels. By judging the visual boundary of the galaxies, I was using a crude Isophotal definition of galaxy size. Figure 9 (pg. 17) shows a typical galaxy image during this measurement process, with an elliptical marquee showing the Photoshop measurement area. (The coloured corners in this image are an artefact of the image rotation that brought the ellipse horizontal for measurement by the Photoshop ellipse tool, which cannot trace inclined ellipses.)

Measured data were collected in an Excel spreadsheet for basic organization, and I used the MATLAB program from Mathworks for statistical analysis and data visualization.

Data Analysis

Messier Spirals

To test and rehearse the techniques, I analysed the 21 non-barred Messier spirals (Figure 10). Unfortunately, this sample of 21 galaxies is too small for any pattern to be evident in either the axis ratios (Figure 11, pg. 18) or the calculated inclinations (Figure 12) so I did no further analysis with the Messiers.

Selection of NGC Spirals

For a larger sample, I measured a selection of 100 NGC galaxies. To generate a useable sample, I selected only non-barred Hubble types Sa and later. I further restricted the sample to only galaxies above a threshold apparent major axis length according to the NGC/IC Project catalogue (Erdmann undated) in order to have images large enough for convenient measurement. I then sorted the list into random order and selected the first 100. Each of these galaxies was measured using Photoshop as described above. Finally, while measuring, I dropped any galaxies whose images showed obvious distortion from interactions. The results are shown in Figure 13 (pg. 19).

Plotting a number of distribution histograms for these data, we first note, in Figure 14, that the measured Axis ratios are not uniform, but display a central tendency which might be normal in a larger sample, except for an apparent outlier at ratio=1. This is good news, as normal axis ratios would indicate selection bias toward random ratios not random inclinations, as discussed above, while normal ratios should approach the predicted arccosine distribution of inclinations. Figure 15 (pg. 20) shows the distribution of the directly-calculated inclinations and markers showing the distribution of an artificially-generated arccosine curve. The sample is small, but one can see a tendency to follow the cosine curve, with two exceptions: There are outliers of incorrect counts of galaxies in the 10°-40° range and, worse, there seem to be too few edge-on galaxies. In uncorrected data, this is not surprising, because edge-on galaxies would have zero thickness, and be undetected.

Hubble's approach for modelling disk thickness with $\cos^2\theta = \frac{(b/a)^2 - q_0^2}{1 - q_0^2}$ would better represent the end points on this curve, especially the 90° edge-on case, but will not address the gaps and irregularities in the middle of the distribution curve. As a sample, Figure 16 (pg. 21) shows the Tully correction, using a fixed 0.20 thickness for the ellipsoid disks. Ignoring the outlier at 50°, this is a closer fit. Very thin ellipses have been classified as ellipsoid disks viewed edge-on, so the 90° distribution is more in line with the predicted curve.

There are still a number of irregularities in these data, however, which I attribute to poor-quality data in my coarse measurements, so I decided to move on to analysis of a statistically significant set of uniformly-measured data from online catalogues.

Catalogue Data

To analyse a large number of consistently and accurately measured spirals, I extracted spiral galaxies from the Principal Galaxy Catalogue (PGC 2003). As with the NGC data above, I selected only non-barred Sa and later type galaxies. To assure relatively accurate data, I eliminated from the sample any galaxies whose error in diameter measurement exceeded 30%, or where any of the important data fields had nonsensical values (such as negative diameters). The result was a sample of 36,368 spirals. PGC, like many catalogues, gives the log of the axis ratio, not the actual axis dimensions, so I calculated the ratios. Figure 17 (pg. 21) shows the first few lines of the resulting list as an example.

The log(axis ratio) figures (Figure 18) roughly follow a log-normal distribution, indicating a distribution of ratios with a central tendency, but we see the ratio distribution is too lopsided and abrupt for a pure Normal fit (Figure 19). Nevertheless, this lead me to expect a good approximation to the arccosine curve seen above for the calculated inclinations.

Calculating the apparent inclinations, we see in Figure 20 (pg. 23) a curve roughly following the predicted arccosine distribution except, again, for an absence of edge-on

(90°) cases. The various q_0 correction schemes discussed above are designed to address these end conditions, so I tested the effect of each.

The basic correction used by Tully and Fisher (1977) uses a fixed value of 0.2 for q_0. Figure 21 (pg. 23) shows this correction yields a distribution still roughly following the arccosine, except for falling off in the last 20 or 30 degrees, and for a large outlier at 90° (edge-on). The outlier at 90° is not surprising since this correction equates all galaxies narrow than 0.2 to edge-on; even if they truly were merely highly-inclined. With this adjustment, 4,246 galaxies in our sample of 36,368 were classified as having an inclination of exactly 90°.

Two methods to apply different q_0 correction values for different galaxy morphological types have been proposed by Haynes and Giovanelli (1984) and Nedyalkov (1993). Figure 22 and Figure 23 (pg. 24) show the distributions that result from applying these corrections to the PGC sample galaxies. Tully's large hump at 90° is spread to the left, across the central tendency hump. Visually, I find the Haynes correction yields a more continuous distribution, except for the now insufficient number of edge-on 90° galaxies.

We can now see the reason for an additional suggested correction. Tully and Fisher (1977) found that the visual observations presented as being slightly too face-on. Aaronson and Mould (1980) agreed; by comparing inclinations calculated from visual data in the RC2 catalogue with radio-based calculations, they found a "small but significant systematic difference", and recommended that all visually-calculated inclinations be increased by a fixed 3° (holding anything exceeding 90° to 90°).

Applying this additional 3° shift to the Haynes-corrected inclinations brings the distribution much closer to the theoretical arccosine, as shown in Figure 24 (pg. 25). Even in this case, there are slight differences between the galaxy distribution and the arccosine reference, but it is clearly closely following that shape, enough that I am prepared to call this a visual match. Plotting the probability distributions of the inclinations and the theoretical arccosine on a quantile-quantile graph shows that the distributions are virtually identical for inclinations greater than about 25° (Figure 25, pg. 25).

Numerically, it is not a good match. Ryden (2005) recommends using the Kolmogorov-Smirnov test to test if two samples appear to come from the same distribution. Using this test in MATLAB to compare the 3°-shifted, Haynes-corrected inclinations to the artificially-generated arccosine sample gave a probability of match near zero, and a KS-test value of 0.1, a very poor match.

H_0 Conclusion

Based solely on the graphic analysis of inclination distributions, there would appear to be good support for the hypothesis that spiral galaxies are round disks randomly oriented in space, with the ellipses we observe being projection effects, especially when the Haynes or Nedyalkov morphology-based corrections for intrinsic disk thickness are used.

Numerically, however, I have been unable to find a match considered statistically significant, due to remaining deficiencies near the face-on end of the distribution.

Most researchers are finding results inconsistent with these, that the distribution of observed spirals is consistent with the galaxies having a small intrinsic ellipticity (references below). Such ellipticities would be expected to present themselves as differences in the frequency of face-on and edge-on inclinations, and may be contributing to the edge deficiencies visible in my distributions.

Limitations

Some caution should accompany the conclusions from this graphic study, as several limitations may affect these analyses.

First, nearly any visually-selected sample of galaxies will suffer from the Malmquist effect: galaxies with larger diameters and higher luminosities are overrepresented (Nedyalkov 1993). Burstein and Haynes (1991) warn that selection (by diameter or luminosity) will determine the inclinations found. While this study should be independent of apparent diameter, it may be biased by selecting higher luminosities, since edge-on galaxies will be over- or under- represented depending on the optical depth of typical galaxies (Ryden 2005).

This dependence of surface brightness on optical depth is an old debate. Authors were pointing out the effects of transparency or opacity of galaxies on their apparent luminosity before Hubble's study (Opik 1923) and even in the last twenty years, have taken conflicting positions on whether galaxies are largely opaque (Valentijn 1990), transparent (Barnes and Sellwood 2003), or somewhere in between (Huizinga and Albada 1992).

My initial Messier sample certainly suffered from this effect, as the Messiers consist of only those large and bright spirals that were easily visible with early observing equipment. The NGC catalogue, on the other hand, was more complete and the PGC catalogue is complete down to a given limiting magnitude. Even when samples are complete, the morphological types of small and dim galaxies may be misclassified if important telltale structural features are not clearly visible.

The slight under-representation of edge-on galaxies in Figure 24 may be indicative of the prevailing feeling that spiral galaxies are semi-transparent, with dust extinction reducing their surface brightness and causing them to be under-selected them in magnitude-limited samples.

Second, this study is based on measurement of the visible dimensions of galaxies, and there are several problems with this approach. Barnes and Sellwood (2003) find that seeing conditions bias elliptical isophotes towards being perceived as round, and Rudnick and Rix (1998) remind us that when we measure visible wavelengths, we are measuring the ellipticity of the visible minority of the material in a galaxy, not necessarily the

ellipticity of its mass distribution. Ryden (2004) poetically calls this "measuring the ellipticity of starlight".

I certainly introduced error of this nature in my measured samples. By hand-fitting an ellipse to a galaxy image, I was doing a crude isophotal size measurement using an aesthetic, rather than an objectively measured, sense of where galactic brightness fell off to a given extent. I was surprised at the variation between some of my measured dimensions and the published dimensions in the NGC catalogue. Often our measures agreed within a few percent, but sometimes they disagreed by as much as 20 or 30%, sometimes on galaxies that appeared no different than those which measured accurately. Clearly the dimensions published in catalogues were measured with some technique more discriminating than my visual inspection of an image.

Finally, the physical structure of spiral galaxies can be a source of error. As already pointed out, our modelling of the thickness of the galaxy as a single ellipsoid is a simplification, and the central bulge can be a source of measurement error (Ma, Song et al. 2000). Worse, the presence of open spiral structure can cause perceptual errors varying with inclination; we tend to underestimate the inclination of face-on galaxies (Aaronson, Huchra et al. 1979). Spiral structures have been blamed for measurement uncertainties on the order of 5 degrees (Barnes and Sellwood 2003).

Again, this may explain the slight under-representation of edge-on galaxies in my results. I avoided certain physical structure errors by rejecting galaxies with obvious signs of interaction, such as bridges to nearby neighbours or major distortions. However I probably misclassified at least some tidal tails as open spiral arms, or vice versa, and I probably perceived certain edge-on galaxies as too thick when they had an abnormally large or bright central bulge.

Alternate Hypothesis: Ellipticity

Visually favouring, but numerically unable to support, the hypothesis that spiral galaxies are randomly inclined round disks, I was interested in trying to detect evidence of their elliptical shapes.

Many researchers have studied this question and concluded the data are consistent with galaxies having slightly elliptical shapes. For ellipsoid solids, *Ellipticity*, or *flatness* is measured as $f = 1 - b/a$. (Elliptical orbits, on the other hand, are usually measured by *eccentricity*, which is related to ellipticity by $e^2 = 2f - f^2$.) Lambas & Maddox (1992) and Andersen & Bershady (2001) both find evidence for ellipticity of approximately 0.1. Ryden (2004), after an combined analysis using photographic and kinematic methods, finds the best fit is with a normal distribution of ellipticities centred around f=0.15.

Not all researchers agree. Barnes & Sellwood (2003), for example, find "no evidence of intrinsically elliptical disks", and argue that various measurement uncertainties can account for all the variations found in the measured data.

Simulation

It was evident that analysis of observational data for consistency with elliptical structures required a level of math and computing capacity well beyond me (Lucy 1974), (Noerdlinger 1979). Instead, I decided to perform a simple simulation, by generating a large sample of galaxies incorporating slight ellipticity in their random dimensions, rotating them randomly in space, and then analysing them in the same manner as the catalogue data, to compare the results. Distributions of my simulated galaxies similar to the distributions of the catalogue data would be evidence in support of ellipticity.

The first problem that presented in this simulation was the geometry of how to rotate elliptical galaxies randomly in space. Circular galaxies, being axisymmetric, need only be rotated on one axis to generate any possible observed ellipse (ignoring position angle). Elliptical galaxies, on the other hand, need to be treated in two dimensions since there *is* a visual difference between rotation on the long and short axes.

Consider first the case of a flat elliptical disk of zero thickness. Figure 26 (pg. 26), shows how this disk can be rotated twice, once by a random amount along the major axis (which changes the length of the minor axis), then by a random amount along the minor axis (which changes the length of the major axis). A third rotation, on the plane of the page, would orient the resulting ellipse at a random position angle. These 3 rotations are sufficient to transform any real disk into the projection seen at any random orientation in the sky. Continuing with our assumption that position angles can be safely ignored, I ignored the 3rd rotation, and kept all the ellipses "horizontal".

Given initial dimensions a and b, the transformations for flat thin disks would be

(1) Rotate on a axis by angle θ_a $\qquad b' = b \cdot \cos\theta_a$

(2) Rotate on b axis by angle θ_b $\qquad a' = a \cdot \cos\theta_b$

To account for the disks being ellipsoid, not flat and infinitely thin, I rewrote the terms of the corrected Hubble formula $\cos^2\theta = \dfrac{ratio^2 - q_0^2}{1 - q_0^2}$ as

$$ratio = \sqrt{\cos^2\theta(1 - q_0^2) + q_0^2}$$

Equation 3

So the complete set of transformations to rotate the ellipsoid in space became:

(1) Rotate on a axis by angle θ_a (shortening b axis, preserving a axis)

$$a' = a$$

$$b' = b \cdot \sqrt{\cos^2\theta_a(1 - q_0^2) + q_0^2}$$

(2) Rotate on b axis by angle θ_b (shortening a axis, preserving new b

$$a'' = a' \cdot \sqrt{\cos^2\theta_b(1 - q_0^2) + q_0^2}$$

axis)

$$b'' = b'$$

To test the hypothesis H_1 that observations are consistent with elliptical disks randomly oriented in space, I generated 3000 ellipses with a uniformly random major axis between 1 and 10, and with a specified average ellipticity (e.g. 0.15) and some variation of ellipticity around this mean. Each was randomly assigned a Hubble morphological type, with the Hubble types distributed in the same percentages as was found in the PGC data. Using the Nedyalkov q_0 corrections based on Hubble type, the ellipsoids were rotated in space by two random angles, using the transformations above, generating apparent major and minor axis lengths. Finally, I plugged these axes into the same analysis used earlier for the measured and catalogue data. Figure 27 (pg. 26) shows a sample of the rotation calculations, and Figure 28 shows a sample of the calculated inclinations, for these simulated galaxies.

I repeated this test with several ellipticities, as follows. (The plus-minus ellipticity variances were arbitrary, except for the figure associated with Ryden. Others were chosen to be about half the ellipticity.)

Ellipticity	**Ellip +/1**	**Reference**	**Figure**	**Comments**
0.05	0.02		Figure 29	
0.1	0.05	Andersen	Figure 30	
0.15	0.08	Ryden	Figure 31	
0.20	0.1		Figure 32	
0.25	0.12		Figure 33	

Table 1: Simulations with Various Ellipticities

Visually inspecting the distributions in these figures, it is evident that they follow the same general shape as the distribution for the Haynes- and Nedyalkov- corrected inclinations in the large PGC sample (Figure 22, Figure 23). However, the fit is not exact – the simulated data have higher distributions at inclinations of 20 to 40 degrees than the real data. A Kolmogorov-Smirnov test confirms what is visually evident: the real and simulated data, while similar, are not from the same sample distribution: a two-sample KS test of the visually closest, the Nedyalkov-corrected real data (Figure 23, pg. 24) and the ellipticity 0.15 simulation (Figure 31, pg. 28) give a KS p-value near 0, and a KS test statistic of 0.17 at 5% significance.

Conclusions

I conclude, based on my own measured samples and on analysis of catalogue data, that spiral galaxies appear, to first approximation, to be round disks randomly inclined to the observer. Minor variances in the two samples, however, prevents a numerical match of statistical significance. Intuitively, over-abundance or scarcity of ellipses at the extremes

(face-on and edge-on) might be evidence in favour of the prevailing "slightly elliptical" hypothesis.

At a more sophisticated level, a literature search shows that most researchers feel that spiral galaxies are not generally round, but exhibit a mild ellipticity. The degree of ellipticity is still uncertain, but values around 0.1 or 0.2 seem likely.

I attempted to reconcile the "elliptical disk" hypothesis with my calculated data by comparing the distribution to the distribution of a simulated universe containing randomly inclined disks with the hypothesised ellipticities. Again, while the visual display of these results suggests a general agreement, a detailed statistical analysis rejects the two distributions as being equivalent. I attribute this failure to errors in my simulation, since my method for generating elliptical ellipsoids and rotating them in space was crude, and I believe that a more capable simulation would find the elliptical-disk theory to be compatible with these observed data.

References

Aaronson, M., J. Huchra, et al. (1979). "The infrared luminosity/H I velocity-width relation and its application to the distance scale." Astrophysical Journal **229**: 1-13.

Aaronson, M., J. Mould, et al. (1980). "A distance scale from the infrared magnitude/H I velocity-width relation. I - The calibration." Astrophysical Journal **237**: 655-665.

Andersen, D. R., M. A. Bershady, et al. (2001). "A Measurement of Disk Ellipticity in Nearby Spiral Galaxies." Astrophysical Journal **551**: L131-L134.

Barnes, E. I. and J. A. Sellwood (2003). "Uncertainties in Spiral Galaxy Projection Parameters." The Astronomical Journal **125**: 1164-1176.

Binney, J. and G. de Vaucouleurs (1981). "The apparent and true ellipticities of galaxies of different Hubble types in the Second Reference Catalogue." Monthly Notices of the Royal Astronomical Society **194**: 679-691.

Burstein, D., M. P. Haynes, et al. (1991). "Dependence of Galaxy Properties on Viewing Angle." Nature **353**(6344): 515-521.

Disney, M. (1990). "Are Spiral Galaxies Opaque?" Nature **346**(6280): 105-106.

Erdmann, B. (undated). The NGC/IC Project: Historically Corrected Catalogue Data for, and DSS Images of, NGC/IC Objects.

Eshbach, O. W. (1936). Handbook of Engineering Fundamentals. New York, John Wiley & Sons.

Haynes, M. P. and R. Giovanelli (1984). "Neutral hydrogen in isolated galaxies. IV - Results for the Arecibo sample." The Astronomical Journal **89**: 758-800.

Hubble, E. P. (1926). "Extragalactic Nebulae." Astrophysical Journal **64**: 321-369.

Huizinga, J. E. and T. S. v. Albada (1992). "Extinction in SC galaxies - an analysis of the ESO-LV data." Monthly Notices of the Royal Astronomical Society **254**: 677-685.

Lambas, D. G., S. J. Maddox, et al. (1992). "On the true shapes of galaxies." Monthly Notices of the Royal Astronomical Society **258**: 404-414.

Lucy, L. B. (1974). "An iterative technique for the rectification of observed distributions." The Astronomical Journal **79**: 745-+.

Ma, J., G. Song, et al. (2000). "Dependence of Spiral Galaxy Distribution on Viewing Angle in RC3." ArXiv Astrophysics e-prints.

Nedyalkov, P. L. (1993). "Effect of the inclination of spiral galaxies on their fundamental observational characteristics." Astronomy Letters **19**: 115-123.

Noerdlinger, P. D. (1979). "The intrinsic flattening of galaxies." Astrophysical Journal **234**: 802-809.

Opik, E. (1923). "On the planes of the spiral nebulae." The Observatory **46**: 51-52.

PGC (2003). Principal Galaxy Catalog 2003, NASA.

Rood, H. J. and W. A. Baum (1967). "Photographic brightness profiles of Coma Cluster galaxies. I. Catalogue of program galaxies." The Astronomical Journal **72**: 398-406.

Rudnick, G. and H.-W. Rix (1998). "Lopsidedness in Early-Type Disk Galaxies." The Astronomical Journal **116**: 1163-1168.

Ryden, B. S. (2004). "The Ellipticity of the Disks of Spiral Galaxies." Astrophysical Journal **601**: 214-220.

Ryden, B. S. (2005). "The Intrinsic Shape of Spiral Galaxies in the 2MASS Large Galaxy Atlas." Astrophysics, from http://arxiv.org/abs/astro-ph/0512377.

Sandage, A., K. C. Freeman, et al. (1970). "The Intrinsic Flattening of e, so, and Spiral Galaxies as Related to Galaxy Formation and Evolution." Astrophysical Journal **160**: 831-+.

Trujillo, I., C. Carretero, et al. (2006). "Detection of the Effect of Cosmological Large-Scale Structure on the Orientation of Galaxies." Astrophysical Journal **640**: L111-L114.

Tully, R. B. (1972). "Inclination corrections to the optical luminosities and diameters of galaxies." Monthly Notices of the Royal Astronomical Society **159**: 35P-+.

Tully, R. B. and J. R. Fisher (1977). "A new method of determining distances to galaxies." Astronomy & Astrophysics **54**: 661-673.

Valentijn, E. A. (1990). "Opaque spiral galaxies." Nature **346**: 153-155.

Figures

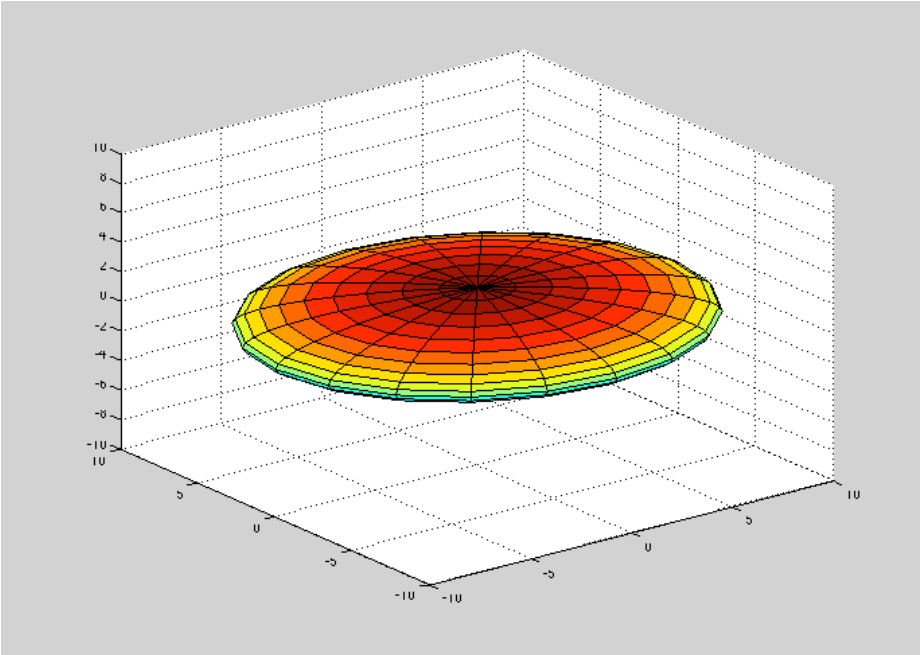

Figure 3: Ellipsoid Seen from Above

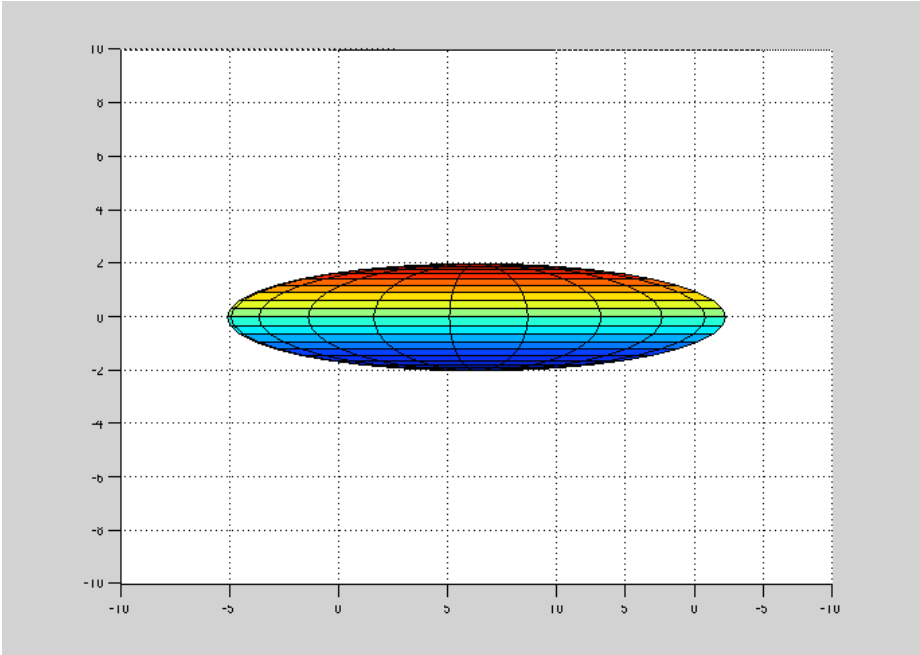

Figure 4: Ellipsoid Edge-On, Showing Thickness

Hubble	Haynes	Nedyalkov
Dwarf	0.1	0.1
Irr	0.1	0.1
Pec	0.175	0.1
S0	0.23	0.175
S0a	0.23	0.175
Sa	0.23	0.175
Sab	0.2	0.14
Sb	0.175	0.14
Sbc	0.14	0.103
Sc	0.103	0.1
Scd	0.1	0.1
Sd	0.1	0.1
Sdm	0.1	0.1
Sm	0.1	0.1

Figure 5 : Galaxy Thickness q_0 Corrections

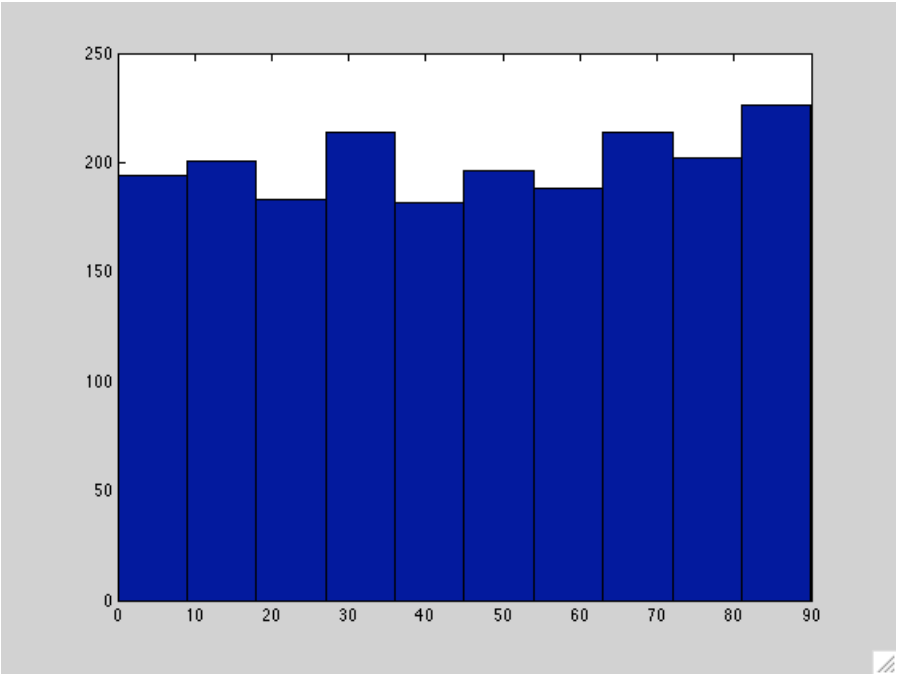

Figure 6: Distribution of Random Inclination Angles

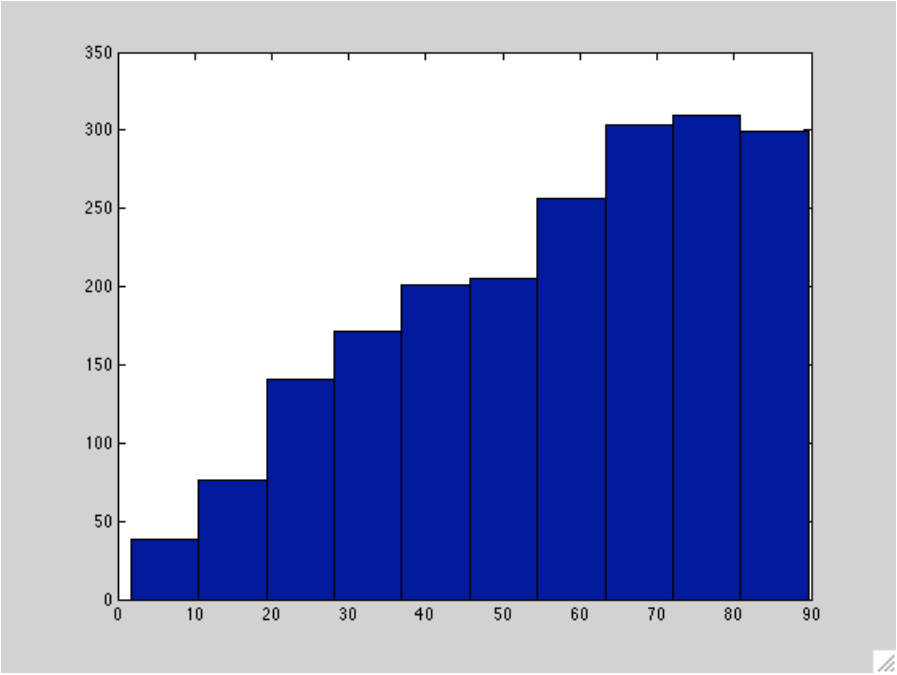

Figure 7: Angles from Random Axis Ratios

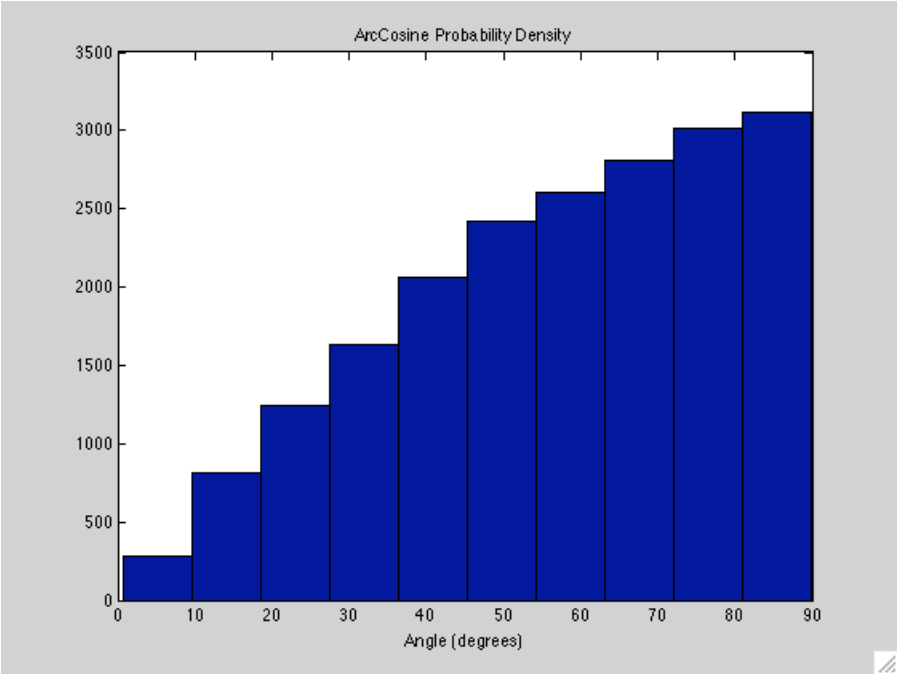

Figure 8: Arccosine probability density

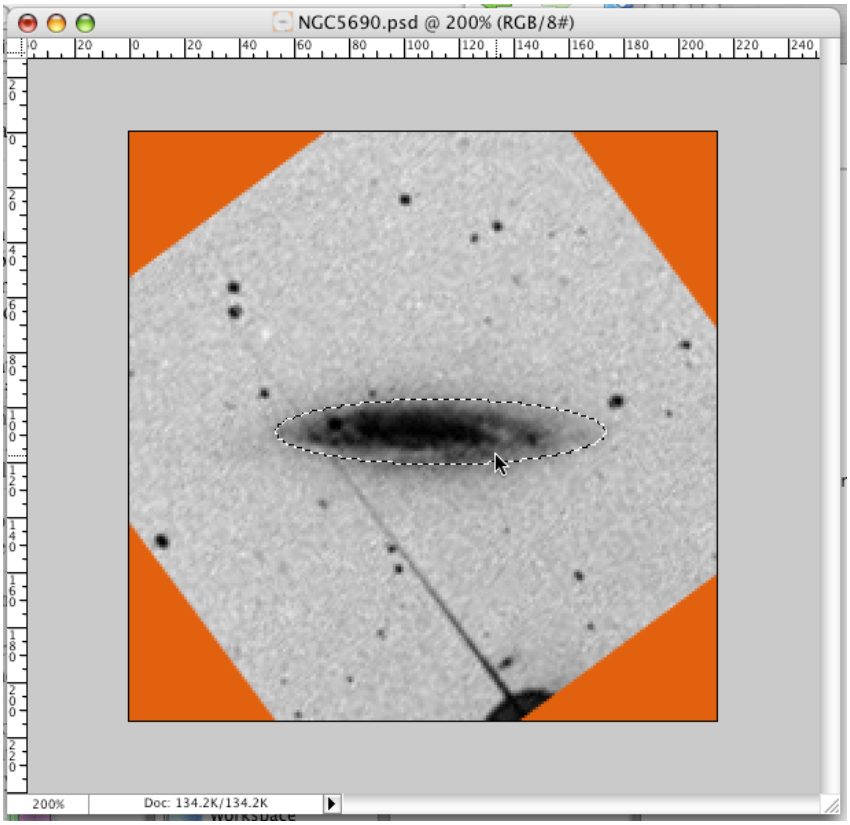

Figure 9: Measuring Ellipse with Photoshop

M#	Type	Measured Major Axis	Measured Minor	Measured ratio	Uncorrected Inclination Deg	dV q-corr	Corrected Tully	Corrected Tully+3	Corrected dV
31	Sb	246.25	86.8	0.35248731	69.36047424	0.14	72.660758	75.66075801	70.834386
33	Sc	652	460	0.705521472	45.12831158	0.103	53.479116	56.47911583	52.33655
51	Sc	432	266	0.615740741	51.99423643	0.103	51.933515	54.93351509	50.851648
63	Sb	208	107	0.514423077	59.04109956	0.14	54.73561	57.73561032	53.896818
64	Sb	276	159	0.576086957	54.82421199	0.14	56.19596	59.19596007	55.31114
65	Sa	378	110	0.291005291	73.08184909	0.14	90	90	82.763498
66	Sb	386	161	0.417098446	65.34846472	0.14	75.814115	78.8141152	73.610576
74	Sc	432	408	0.944444444	19.18813645	0.103	21.812777	24.81277697	21.470014
77	Sb	236	182	0.771186441	39.53944994	0.14	31.715382	34.71538234	31.3458
81	Sb	544	390	0.716911765	44.19990491	0.14	63.828105	66.82810504	62.634022
88	Sc	156	74	0.474358974	61.68237888	0.103	56.884845	59.88484521	55.592537
90	Sb	315	144	0.457142857	62.79710559	0.14	64.008011	67.00801107	62.804786
94	Sb	400	319	0.7975	37.10797126	0.14	67.240804	70.24080392	65.852396
96	Sa	106	71	0.669811321	47.94749588	0.14	49.528222	52.52822239	48.830866
98	Sb	248	50	0.201612903	78.36870691	0.14	73.940891	76.94089077	71.97588
99	Sc	135	114	0.844444444	32.38753853	0.103	27.876654	30.87665405	27.424054
100	Sc	407	372	0.914004914	23.93519542	0.103	31.715382	34.71538234	31.187
101	Sc	400	362	0.905	25.17671694	0.103	0	3	0
104	Sa	464	177	0.381465517	67.57551025	0.14	66.103485	69.10348487	64.785129
106	Sbp	376	202	0.537234043	57.5044541	0.14	67.780199	70.78019931	66.356427
108	Sc	236	58	0.245762712	75.7730879	0.103	90	90	85.916947

Figure 10: Messier Spirals

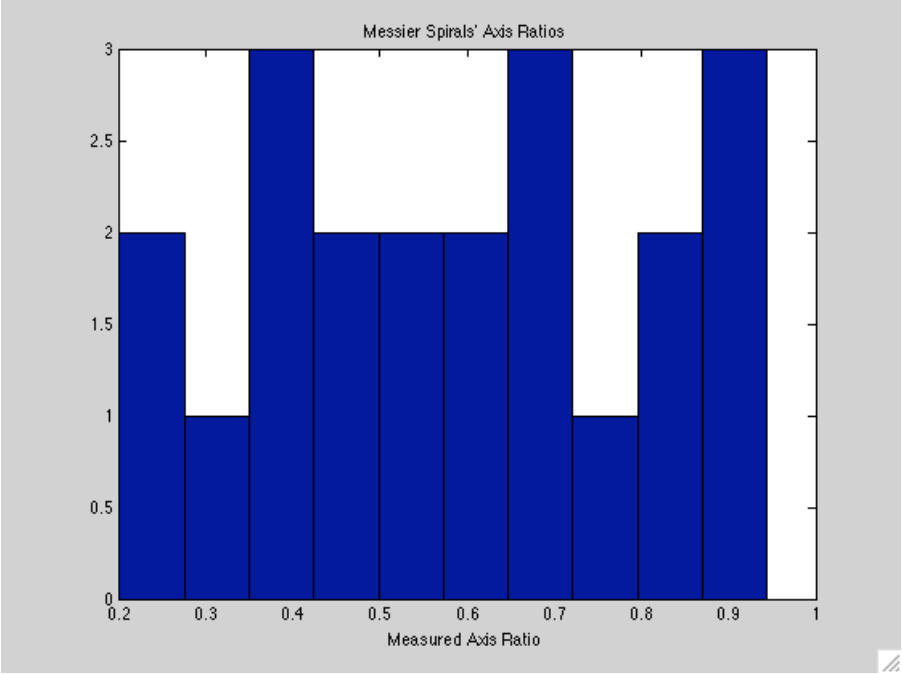

Figure 11: Messier Axis Ratios

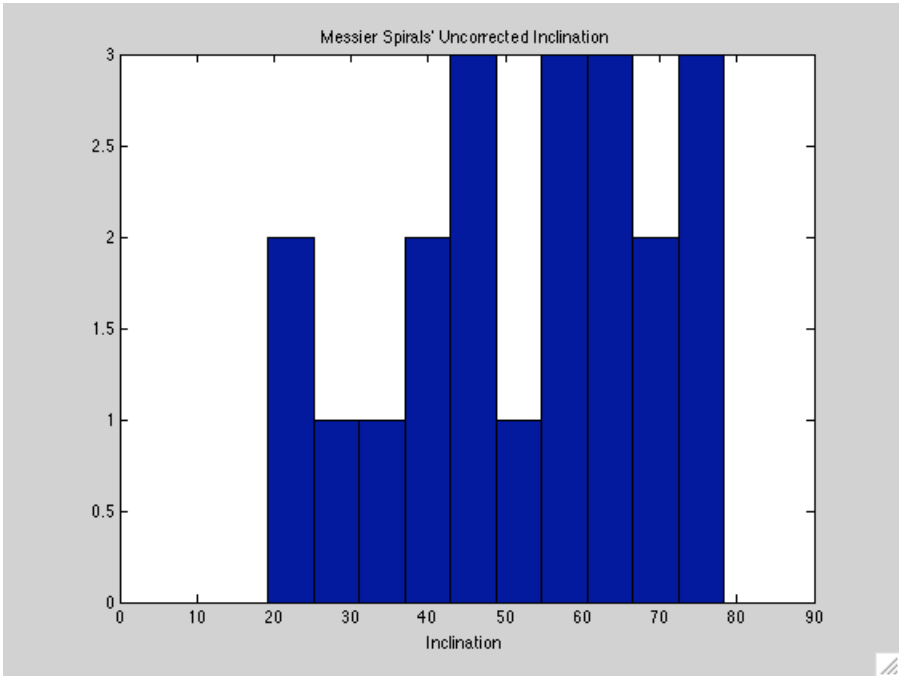

Figure 12: Messier Uncorrected Inclinations

NGC	Type	Meas a	Meas b	Meas ratio	Meas Angle	Haynes q-corr	Corrected Tully	Corrected Tully + shift	Corrected Haynes
4289	Sc	122	10	0.08197	85.298	**0.103**	**90**	**90**	**90**
4356	Sc	87	12	0.13793	82.072	**0.103**	**90**	**90**	**84.70814**
5131	Sa	69	10	0.14493	81.667	**0.14**	**90**	**90**	**87.83126**
4749	Sb	59	11	0.18644	79.255	**0.14**	**90**	**90**	**82.85671**
3795	Scd	61	12	0.19672	78.655	**0.103**	**90**	**90**	**80.29952**
669	Sab	88	18	0.20455	78.197	**0.14**	**87.49159**	**90**	**81.33771**
5690	Sc	120	26	0.21667	77.487	**0.103**	**85.121**	**88.121001**	**78.95162**
2758	Sc	76	17	0.22368	77.074	**0.103**	**84.13191**	**87.131905**	**78.48523**
2613	Sb	253	58	0.22925	76.747	**0.14**	**83.43328**	**86.43328**	**79.43557**
11	Sa	61	14	0.22951	76.732	**0.14**	**83.40212**	**86.402121**	**79.41631**
964	Sab	77	19	0.24675	75.715	**0.14**	**81.51769**	**84.517686**	**78.158**
13	Sab	81	20	0.24691	75.705	**0.14**	**81.50151**	**84.501511**	**78.14649**
4845	Sab	112	32	0.28571	73.398	**0.14**	**77.98028**	**80.980283**	**75.43129**
1956	Sa	80	23	0.2875	73.292	**0.14**	**77.83119**	**80.831185**	**75.3089**
6011	Sb	75	22	0.29333	72.942	**0.14**	**77.34943**	**80.349432**	**74.91023**
4257	Sab	34	10	0.29412	72.895	**0.14**	**77.28524**	**80.285241**	**74.85676**
6313	Sab	44	13	0.29545	72.815	**0.14**	**77.17612**	**80.176124**	**74.76567**
2429	Sbc	52	16	0.30769	72.08	**0.14**	**76.19327**	**79.193267**	**73.9353**
2748	Sbc	96	30	0.3125	71.79	**0.14**	**75.81412**	**78.814115**	**73.61058**
3835	Sab	73	23	0.31507	71.635	**0.14**	**75.61297**	**78.612969**	**73.43739**
54	Sa	47	15	0.31915	71.389	**0.14**	**75.2953**	**78.295299**	**73.16265**
4012	Sb	34	11	0.32353	71.123	**0.14**	**74.95667**	**77.95667**	**72.86819**
803	Sc	92	30	0.32609	70.969	**0.103**	**74.76003**	**77.760034**	**71.87767**
2007	Sc	64	21	0.32813	70.845	**0.103**	**74.60387**	**77.603874**	**71.74748**
2814	Sb	42	14	0.33333	70.529	**0.14**	**74.20683**	**77.206831**	**72.21073**
9	Sb/P	53	18	0.33962	70.146	**0.14**	**73.73097**	**76.730967**	**71.78991**
4877	Sab	94	33	0.35106	69.448	**0.14**	**72.87406**	**75.874057**	**71.02577**
2726	Sa	54	19	0.35185	69.399	**0.14**	**72.81541**	**75.815408**	**70.97319**
7606	Sb	159	62	0.38994	67.049	**0.14**	**70.02301**	**73.023012**	**68.43491**
4300	Sa	51	20	0.39216	66.911	**0.14**	**69.8622**	**72.862202**	**68.28691**
2275	Sab	37	15	0.40541	66.083	**0.14**	**68.90535**	**71.905354**	**67.40286**
6948	Sa	90	37	0.41111	65.725	**0.14**	**68.49456**	**71.494564**	**67.02163**
4456	Sbc	49	21	0.42857	64.623	**0.14**	**67.2408**	**70.240804**	**65.8524**
3898	Sab	99	43	0.43434	64.256	**0.14**	**66.82708**	**69.827077**	**65.46484**
1292	Sc	103	45	0.43689	64.094	**0.103**	**66.64438**	**69.644385**	**64.73228**
1511	Sa	105	46	0.4381	64.018	**0.14**	**66.55827**	**69.558269**	**65.2126**
6719	Sc	67	31	0.46269	62.439	**0.103**	**64.79672**	**67.796718**	**63.03229**
6207	Sc	83	40	0.48193	61.189	**0.103**	**63.41598**	**66.41598**	**61.75066**
834	Sbc	37	18	0.48649	60.89	**0.14**	**63.08818**	**66.088181**	**61.93059**
594	Sbc	39	19	0.48718	60.845	**0.14**	**63.03832**	**66.038323**	**61.88313**
31	Sc	43	21	0.48837	60.766	**0.103**	**62.9525**	**65.952503**	**61.31854**
6632	Sbc	86	43	0.5	60	**0.14**	**62.11443**	**65.114433**	**61.00231**
2446	Sb	55	28	0.50909	59.397	**0.14**	**61.4573**	**64.457302**	**60.37436**
6063	Sc	53	27	0.50943	59.374	**0.103**	**61.43247**	**64.432467**	**59.89538**
7025	Sa	45	23	0.51111	59.262	**0.14**	**61.31101**	**64.311015**	**60.23441**
2	Sab	35	18	0.51429	59.05	**0.14**	**61.08093**	**64.080932**	**60.01419**
5937	Sb	70	37	0.52857	58.091	**0.14**	**60.04221**	**63.042212**	**59.01836**
5696	Sbc	44	24	0.54545	56.944	**0.14**	**58.80655**	**61.806549**	**57.83052**
3860	Sab	47	27	0.57447	54.938	**0.14**	**56.6581**	**59.658096**	**55.75801**
1054	Sbc	33	19	0.57576	54.847	**0.14**	**56.56177**	**59.561771**	**55.6649**
4218	Sa	35	21	0.6	53.13	**0.14**	**54.73561**	**57.73561**	**53.89682**
5939	Sbc	31	19	0.6129	52.2	**0.14**	**53.75068**	**56.750679**	**52.94118**
2958	Sbc	42	26	0.61905	51.753	**0.14**	**53.27818**	**56.278182**	**52.48227**
1069	Sc	50	31	0.62	51.684	**0.103**	**53.20473**	**56.204735**	**52.07324**
2786	Sa	29	18	0.62069	51.633	**0.14**	**53.15151**	**56.151513**	**52.3592**
3197	Sbc	40	25	0.625	51.318	**0.14**	**52.81819**	**55.818188**	**52.03523**
4651	Sc/P	121	77	0.63636	50.479	**0.103**	**51.93352**	**54.933515**	**50.85165**
7764	Sc	91	59	0.64835	49.583	**0.103**	**50.99039**	**53.990392**	**49.94366**
3846	Sbc	37	24	0.64865	49.56	**0.14**	**50.96689**	**53.966892**	**50.23354**
3435	Sb	41	27	0.65854	48.812	**0.14**	**50.18061**	**53.180606**	**49.46719**
5720	Sb	48	32	0.66667	48.19	**0.14**	**49.52822**	**52.528222**	**48.83087**
7519	Sb	51	34	0.66667	48.19	**0.14**	**49.52822**	**52.528222**	**48.83087**
7003	Sbc	40	27	0.675	47.546	**0.14**	**48.85371**	**51.853712**	**48.17253**
789	Sd	25	17	0.68	47.156	**0.1**	**48.44605**	**51.446051**	**47.46851**
7757	Sc	75	51	0.68	47.156	**0.103**	**48.44605**	**51.446051**	**47.48773**
2308	Sab	60	41	0.68333	46.895	**0.14**	**48.173**	**51.173004**	**47.50773**
5744	Sab	48	33	0.6875	46.567	**0.14**	**47.83022**	**50.830224**	**47.17281**
5490	Sc	76	53	0.69737	45.784	**0.103**	**47.01162**	**50.011618**	**46.09951**
706	Sc	47	33	0.70213	45.402	**0.103**	**46.6133**	**49.613296**	**45.7136**
2985	Sb	138	97	0.7029	45.34	**0.14**	**46.54855**	**49.548553**	**45.91965**
1492	Sa	27	19	0.7037	45.275	**0.14**	**46.48087**	**49.480866**	**45.85343**
6824	Sab	61	43	0.70492	45.177	**0.14**	**46.37865**	**49.378649**	**45.75343**
4067	Sb	41	29	0.70732	44.983	**0.14**	**46.17624**	**49.17624**	**45.55538**
7266	Sa	25	18	0.72	43.946	**0.14**	**45.09549**	**48.095493**	**44.49738**
1694	Sc	29	22	0.75862	40.657	**0.103**	**41.67984**	**44.679841**	**40.92089**
1509	Sa	25	19	0.76	40.536	**0.14**	**41.55395**	**44.553949**	**41.02494**
7653	Sb	57	45	0.78947	37.864	**0.14**	**38.78804**	**41.788038**	**38.30806**
6550	Sbc	69	55	0.7971	37.146	**0.14**	**38.04623**	**41.046233**	**37.57877**
1	Sb	56	45	0.80357	36.527	**0.14**	**37.40765**	**40.407654**	**36.95077**
2775	Sab	106	86	0.81132	35.775	**0.14**	**36.63079**	**39.630786**	**36.18653**
5256	Sab/P	18	15	0.83333	33.557	**0.14**	**34.34463**	**37.344628**	**33.93617**
3515	Sbc	31	27	0.87097	29.429	**0.14**	**30.09743**	**33.097434**	**29.75071**
3277	Sab	65	59	0.90769	24.812	**0.14**	**25.35906**	**28.359061**	**25.07538**
7719	Sab	12	11	0.91667	23.556	**0.14**	**24.07259**	**27.072592**	**23.80516**
3149	Sb	74	68	0.91892	23.231	**0.14**	**23.73958**	**26.739582**	**23.47631**
3765	Sc	32	30	0.9375	20.364	**0.103**	**20.80331**	**23.803311**	**20.47789**
6001	Sc	39	37	0.94872	18.429	**0.103**	**18.82281**	**21.822807**	**18.53078**
1363	Sbc	28	27	0.96429	15.359	**0.14**	**15.68366**	**18.683662**	**15.51548**
5978	Sa	28	27	0.96429	15.359	**0.14**	**15.68366**	**18.683662**	**15.51548**
6484	Sb	59	57	0.9661	14.961	**0.14**	**15.27697**	**18.276968**	**15.11336**
7132	Sc	30	29	0.96667	14.835	**0.103**	**15.14828**	**18.148275**	**14.91627**
1654	Sa	34	33	0.97059	13.931	**0.14**	**14.2238**	**17.223798**	**14.07195**
6033	Sbc	37	36	0.97297	13.351	**0.14**	**13.63175**	**16.631753**	**13.48648**
7251	Sa	37	36	0.97297	13.351	**0.14**	**13.63175**	**16.631753**	**13.48648**
1219	Sc	37	36	0.97297	13.351	**0.103**	**13.63175**	**16.631753**	**13.42391**
198	Sc	40	39	0.975	12.839	**0.103**	**13.10798**	**16.107976**	**12.9084**
7130	Sa	57	56	0.98246	10.748	**0.14**	**10.97259**	**13.972593**	**10.85643**
7478	Sa	14	14	1	0	**0.14**	**0**	**3**	**0**
6975	Sbc	37	37	1	0	**0.14**	**0**	**3**	**0**
5958	Sc	39	39	1	0	**0.103**	**0**	**3**	**0**

Figure 13: Measured NGC Sample Spirals

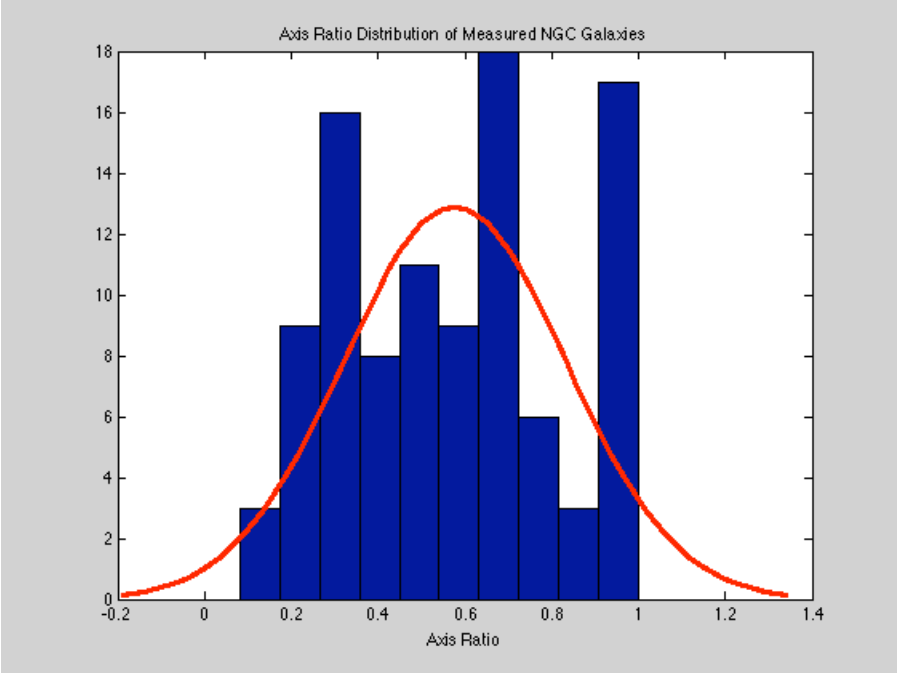

Figure 14: Axis Ratio Distribution of Measured NGCs

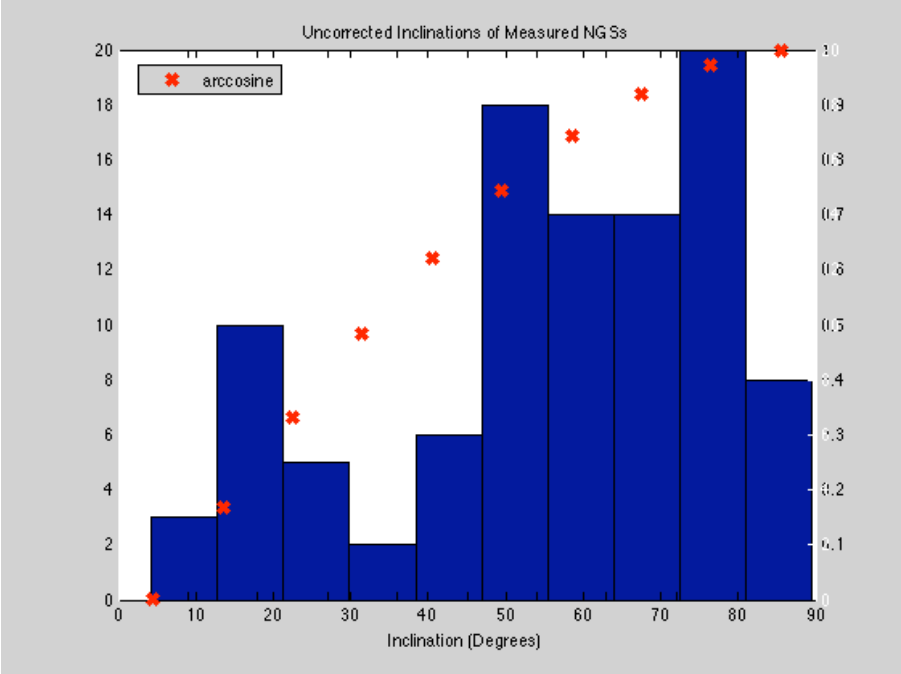

Figure 15: Uncorrected Inclinations of Measured NGCs

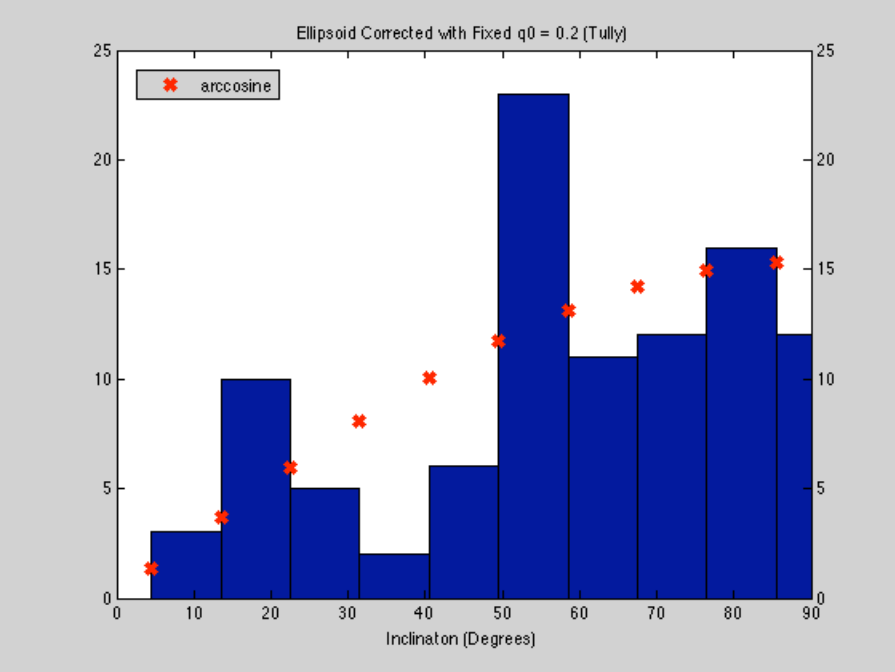

Figure 16: NGC Ellipsoids Corrected with Fixed q_0 = 0.2 (Tully)

name	morph_type	apparent_diam	Diam Error percent	log_axis_ratio	axis ratio (10^x)	Haynes morphed q correction	Nedyalkov morphed q correction	uncorrected inclination	Tully fixed q-corrected inclination	Haynes q-corrected inclination	Nedyalkov q-corrected inclination	Tully fixed corrected with 3°
PGC 83956	Sab	0.47	29.78723404	0.23	0.588843655	0.200	0.140	53.92500665	55.57973267	55.57973267	54.7147329	58.57973267
PGC 94937	Sa	0.54	29.62962963	0.08	0.831763771	0.230	0.175	33.71965147	34.5118672	34.77968672	34.32112052	37.5118672
PGC 38070	Sab	0.78	29.48717949	0.26	0.549540874	0.200	0.140	56.6644793	58.50598788	58.50598788	57.54111225	61.50598788
PGC 2793333	Sab	0.69	28.98550725	0.57	0.26915348	0.200	0.140	74.38609978	79.40676537	79.40676537	76.57550191	82.40676537
PGC 42265	Sab	0.76	28.94736842	0.21	0.616595002	0.200	0.140	51.9320924	53.4670648	53.4670648	52.66575633	56.4670648
PGC 85585	Sab	0.38	28.94736842	0.09	0.812830516	0.200	0.140	35.62659039	36.47783993	36.47783993	36.03604355	39.47783993
PGC 74096	Sab	0.38	28.94736842	0.08	0.831763771	0.200	0.140	33.71965147	34.5118672	34.5118672	34.10085237	37.5118672
PGC 95125	Sab	0.56	28.57142857	0.21	0.616595002	0.200	0.140	51.9320924	53.4670648	53.4670648	52.66575633	56.4670648
PGC 159103	Sa	0.78	28.20512821	0.48	0.331131121	0.230	0.175	70.66255566	74.37436524	75.83114253	73.41030898	77.37436524
PGC 95222	Sa	0.94	27.65957447	0.84	0.144543977	0.230	0.175	81.68912719	90	90	90	90
PGC 75491	Sab	0.58	27.5862069	0.22	0.602559586	0.200	0.140	52.94656472	54.54099093	54.54099093	53.70809365	57.54099093
PGC 73718	Sab	0.40	27.5	0.05	0.891250938	0.200	0.140	26.96913747	27.57195523	27.57195523	27.25949991	30.57195523
PGC 75507	Sab	0.55	27.27272727	0.29	0.512861384	0.200	0.140	59.14538624	61.18419283	61.18419283	60.11304019	64.18419283
PGC 83981	Sab	0.59	27.11864407	0.11	0.776247117	0.200	0.140	39.08176232	40.04796324	40.04796324	39.54613148	43.04796324
PGC 73291	Sab	0.59	27.11864407	0.42	0.380189396	0.200	0.140	67.65458521	70.7312267	70.7312267	69.0845457	73.7312267
PGC 6005	Sa	0.74	27.02702703	0.04	0.912010839	0.230	0.175	24.21526932	24.74774668	24.92713384	24.61978947	27.74774668
PGC 74125	Sab	0.41	26.82926829	0.15	0.707945784	0.200	0.140	44.93197646	46.12309194	46.12309194	45.50336654	49.12309194
PGC 74140	Sab	0.41	26.82926829	0.14	0.72443596	0.200	0.140	43.57805343	44.71307105	44.71307105	44.12280854	47.71307105
PGC 42097	Sa	0.76	26.31578947	0.31	0.489778819	0.230	0.175	60.67395495	62.85124402	63.61966063	62.3145391	65.85124402
PGC 27510	Sab	0.76	26.31578947	0.3	0.501187234	0.200	0.140	59.92142212	62.02871701	62.02871701	60.92047021	65.02871701
PGC 170227	Sa	0.80	26.25	0.16	0.691830971	0.230	0.175	46.22477859	47.47215158	47.8978534	47.17022179	50.47215158
PGC 74124	Sab	0.42	26.19047619	0.08	0.831763771	0.200	0.140	33.71965147	34.5118672	34.5118672	34.10085237	37.5118672
PGC 84783	Sab	0.42	26.19047619	0.03	0.933254301	0.200	0.140	21.05207924	21.50754132	21.50754132	21.27159639	24.50754132
PGC 42560	Sa	0.77	25.97402597	0.4	0.398107171	0.230	0.175	66.54009822	69.43187149	70.49454154	68.70402792	72.43187149
PGC 6533	Sa	0.89	25.84269663	0.53	0.295120923	0.230	0.175	72.83521144	77.20331938	79.04623498	76.03308179	80.20331938
PGC 27778	Sab	0.89	25.84269663	0.35	0.446683592	0.200	0.140	63.46889508	65.94311615	65.94311615	64.63417925	68.94311615
PGC 58588	Sab	0.89	25.84269663	0	1	0.200	0.140	0	0	0	0	3
PGC 19908	Sab	0.89	25.84269663	0.24	0.575439937	0.200	0.140	54.8695529	56.58550584	56.58550584	55.68784137	59.58550584
PGC 35471	Sab	0.89	25.84269663	0.43	0.371535229	0.200	0.140	68.18966997	71.36323133	71.36323133	69.66112635	74.36323133
PGC 2793392	Sab	0.66	25.75757576	0.13	0.741310241	0.200	0.140	42.15685205	43.23579408	43.23579408	42.6749429	46.23579408

Figure 17: Sample from Principal Galaxy Catalogue

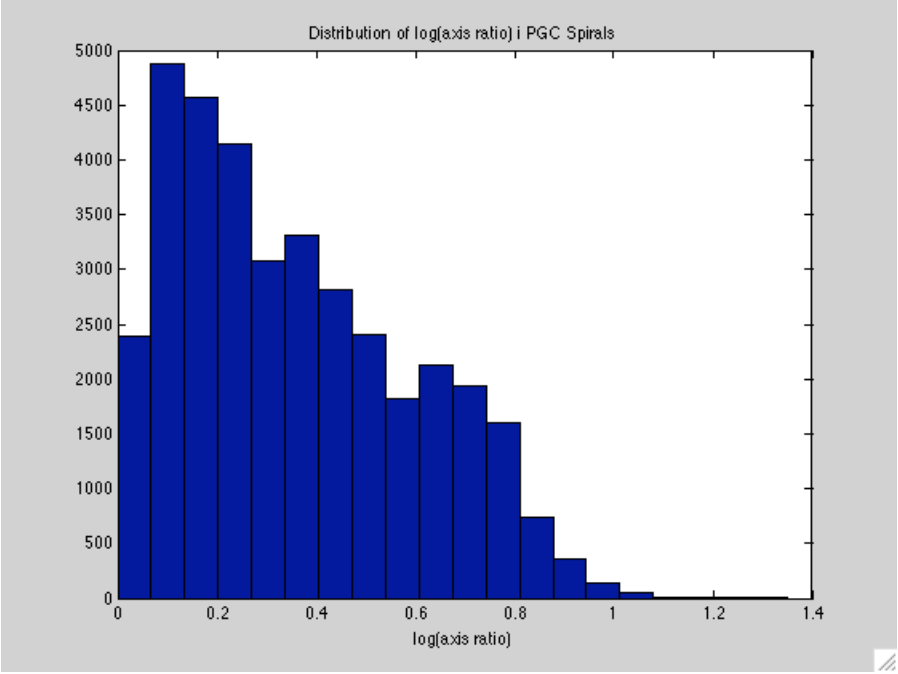

Figure 18: PGC Log(axis ratio) Distribution

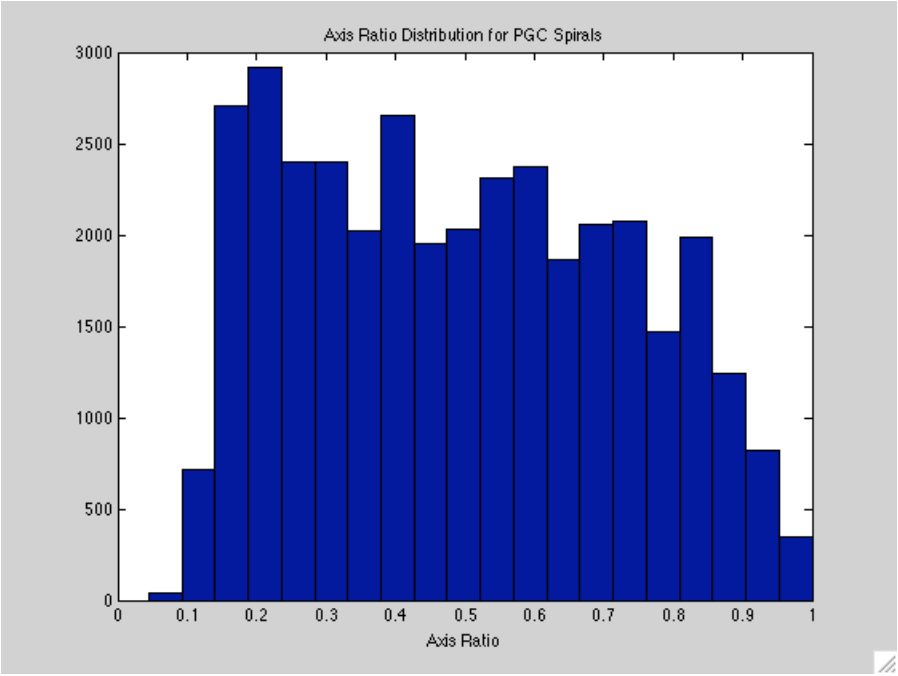

Figure 19: Axis Ratios of PGC Spirals

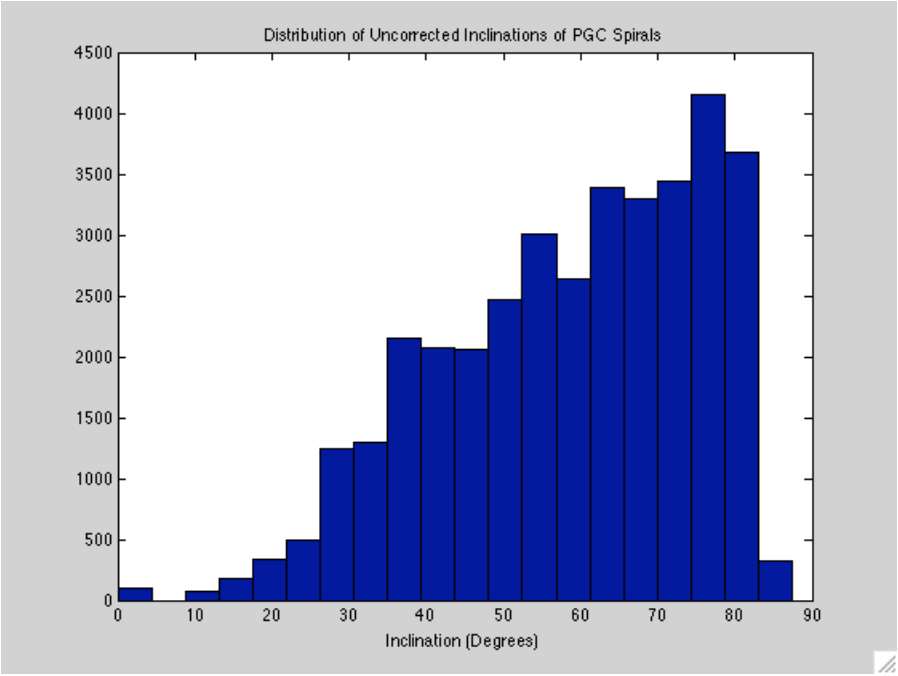

Figure 20: Uncorrected Inclinations of PGC Spirals

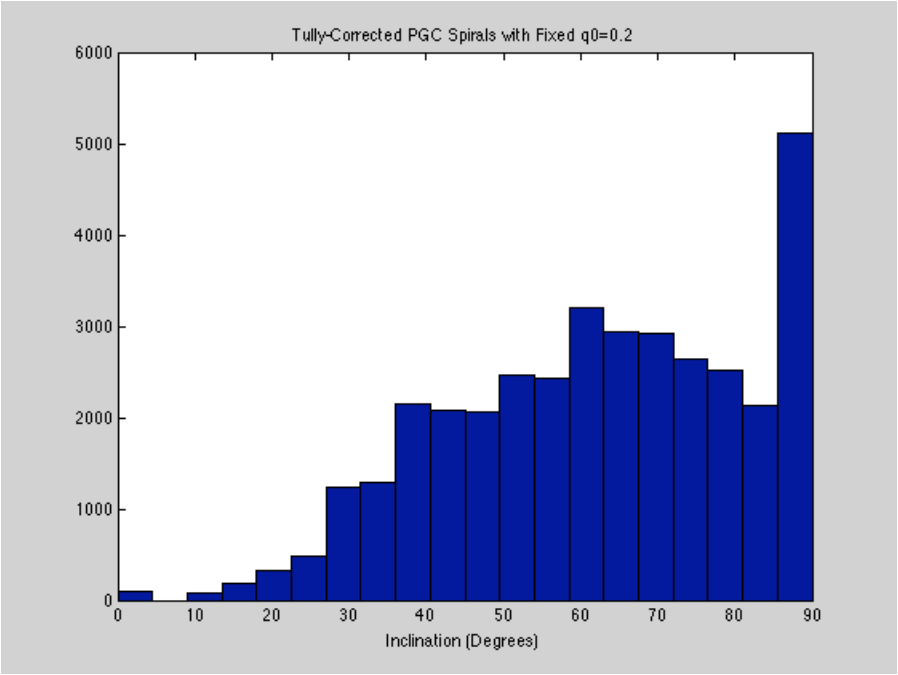

Figure 21: Tully-Corrected PGC Spirals. Fixed q_0=0.2.

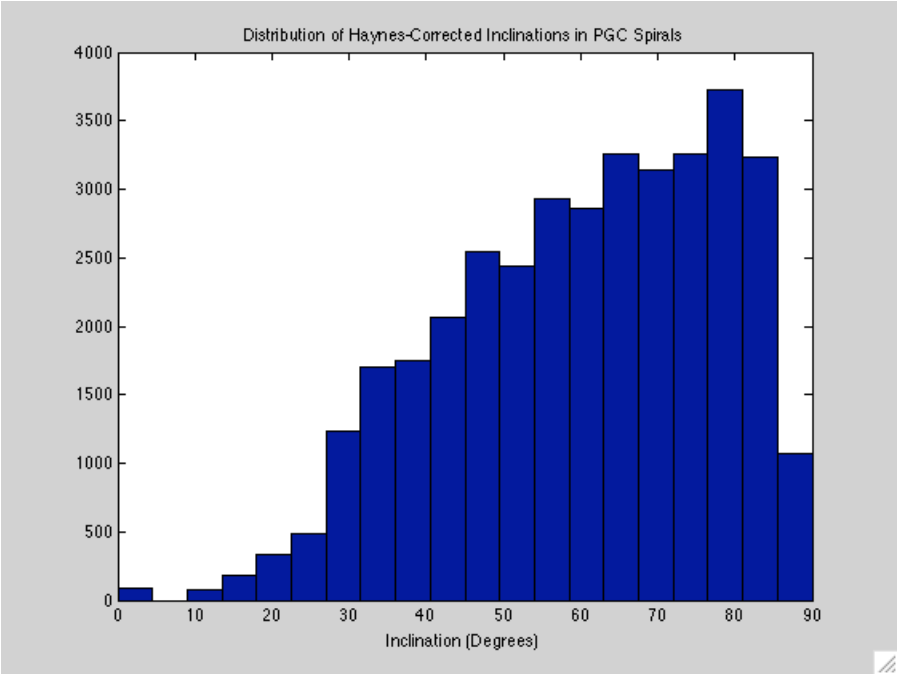

Figure 22: Haynes-Corrected PGC Spirals

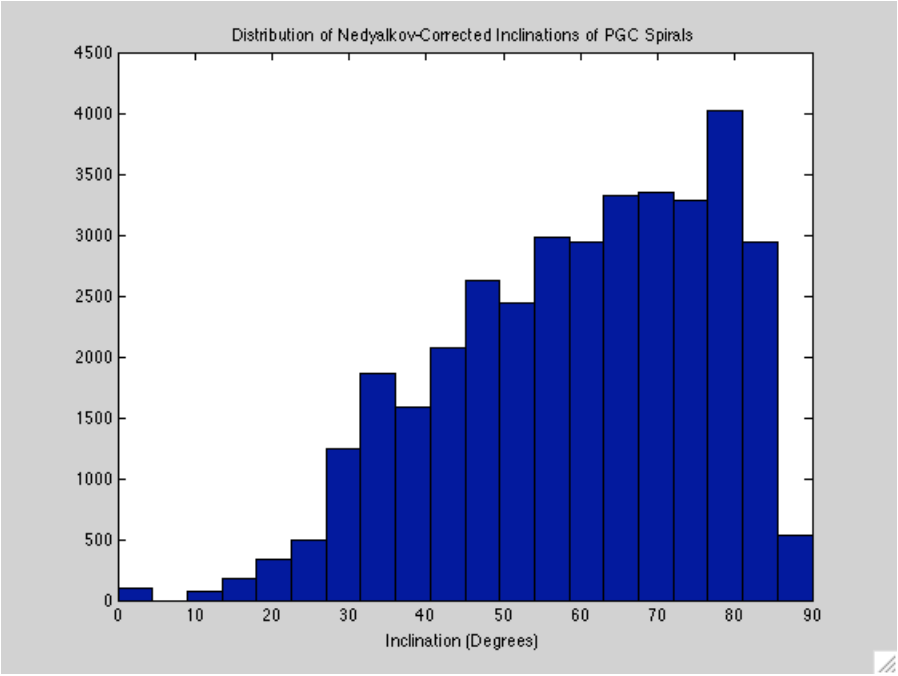

Figure 23: Nedyalkov-Corrected PGC Spirals

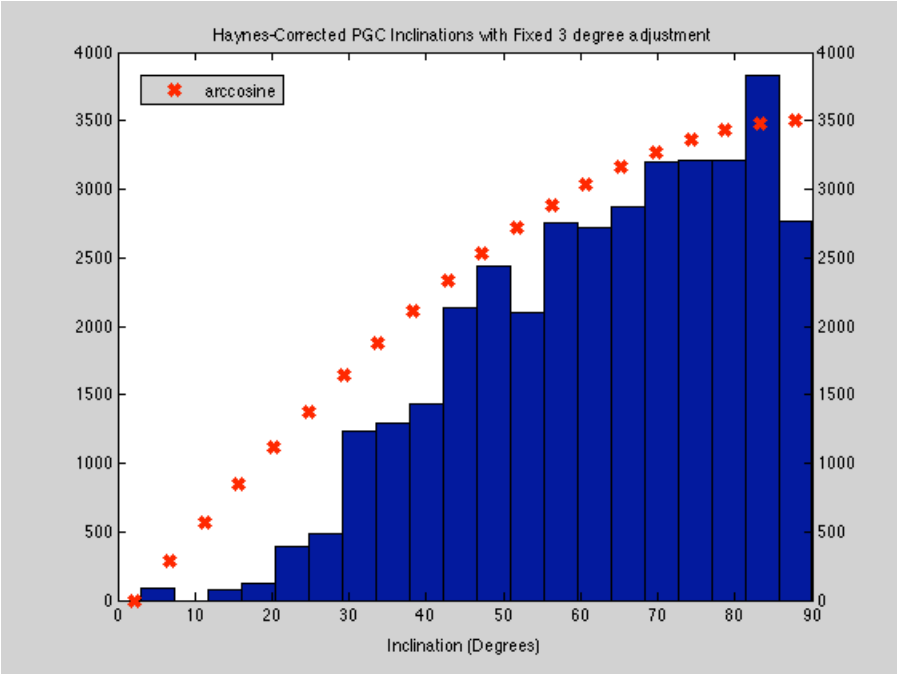

Figure 24: Haynes-Corrected PGC Spirals with 3-degree shift

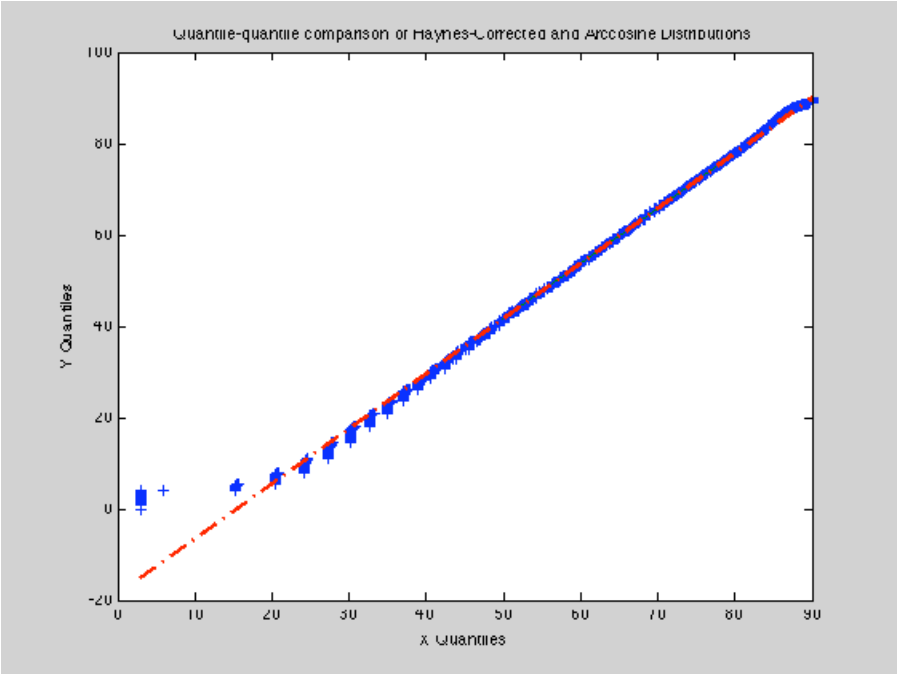

Figure 25: Quantile-quantile comparison of probability distributions

---

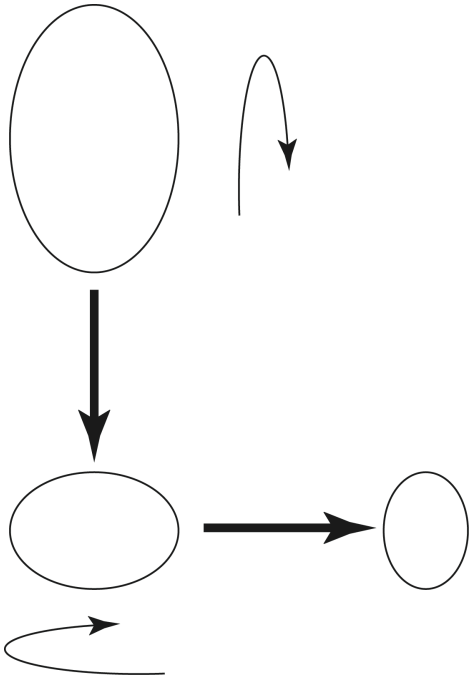

Figure 26: 2-dimensional Rotation of an Ellipse

										Simple rotation with qCorr					
Num	Type	Nedyalkov	Diam	ellipticity	major (a)	minor (b)	Inclination	Rotation		ratio1	a'	b'	ratio2	a''	b''
1	Sc	0.1	1.55138	0.069244	1.5513812	1.4439571	55.535518	25.24746		0.57187	1.55138	0.82576	0.90548	1.40474	0.82576
2	Sc	0.1	9.01688	0.037814	9.0168763	8.6759154	45.759638	54.42189		0.70134	9.01688	6.08476	0.58747	5.29714	6.08476
3	Sc	0.1	4.64446	0.056252	4.6444584	4.3831978	39.289701	53.17663		0.77654	4.64446	3.40373	0.60467	2.80837	3.40373
4	Sbc	0.103	2.12804	0.060499	2.128038	1.9992929	81.068907	56.75411		0.18562	2.12804	0.37111	0.55496	1.18097	0.37111
5	Sc	0.1	2.36363	0.053666	2.3636276	2.2367809	44.423648	73.66776		0.71761	2.36363	1.60513	0.29713	0.70231	1.60513
6	Sb	0.14	3.08829	0.063379	3.0882899	2.8925557	51.2781	71.2393		0.63501	3.08829	1.83679	0.34786	1.07431	1.83679
7	Sb	0.14	9.99723	0.05835	9.997235	9.4138991	36.070668	29.04761		0.81248	9.99723	7.64864	0.87686	8.76613	7.64864
8	Sbc	0.103	2.7466	0.061037	2.7466038	2.5789583	10.430794	39.84805		0.98365	2.7466	2.5368	0.77058	2.11647	2.5368
9	Sc	0.1	2.29829	0.056848	2.2982932	2.1676404	12.408695	24.81263		0.97688	2.29829	2.11752	0.90865	2.08835	2.11752
10	Sc	0.1	9.43953	0.030264	9.4395262	9.1538443	89.947412	42.54783		0.1	9.43953	0.91542	0.73981	6.98345	0.91542
11	Sb	0.14	6.48835	0.035435	6.4883538	6.258442	53.904174	31.91072		0.5999	6.48835	3.75444	0.85209	5.52868	3.75444
12	Sc	0.1	3.02502	0.051084	3.0250244	2.8704942	39.389297	41.30135		0.77545	3.02502	2.22593	0.75414	2.2813	2.22593
13	Sc	0.1	9.66663	0.063922	9.6666334	9.0487233	74.996418	88.83998		0.27631	9.66663	2.50027	0.10201	0.98608	2.50027

Figure 27: 3D Rotation of Simulated Disks with Ellipticity

		Simple rotation with Nedyalkov correction					
Type	q0	dim-1	dim-2	a	b	ratio	inc deg
Sc	0.1	1.404743386	0.825755469	1.404743386	0.825755469	0.587833676	54.39572362
Sc	0.1	5.297139931	6.084755018	6.084755018	5.297139931	0.870559277	29.63958566
Sc	0.1	2.808374832	3.403729664	3.403729664	2.808374832	0.82508751	34.60052919
Sbc	0.103	1.180974934	0.371108751	1.180974934	0.371108751	0.314239312	72.63446217
Sc	0.1	0.70230556	1.605126744	1.605126744	0.70230556	0.437539006	64.65269893
Sb	0.14	1.074306498	1.836788644	1.836788644	1.074306498	0.584883025	55.00333186
Sb	0.14	8.766128058	7.6486389	8.766128058	7.6486389	0.872521922	29.56657587
Sbc	0.103	2.11647222	2.536795093	2.536795093	2.11647222	0.83430949	33.65867199
Sc	0.1	2.088354593	2.117515983	2.117515983	2.088354593	0.986228491	9.568213924
Sc	0.1	6.983454801	0.915422598	6.983454801	0.915422598	0.131084488	85.11360152
Sb	0.14	5.528677678	3.754440151	5.528677678	3.754440151	0.679084651	47.84750365
Sc	0.1	2.281299104	2.225933461	2.281299104	2.225933461	0.975730652	12.71357558
Sc	0.1	0.986079802	2.500271714	2.500271714	0.986079802	0.394389056	67.45415455

Figure 28: Inclinations Calculated from Simulated Galaxies

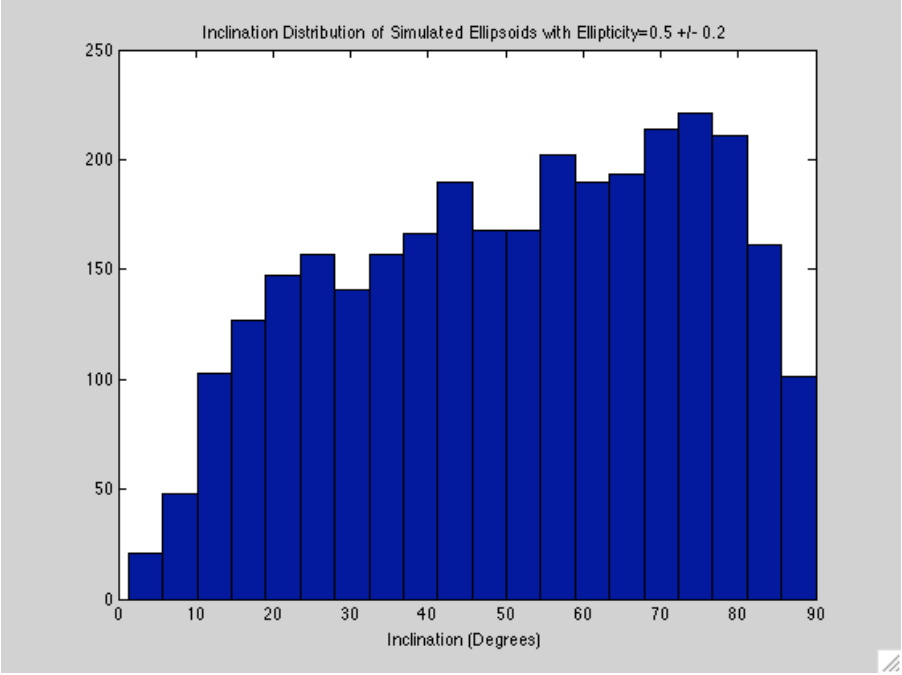

Figure 29: Inclinations of Simulated Galaxies with Ellipticity 0.05

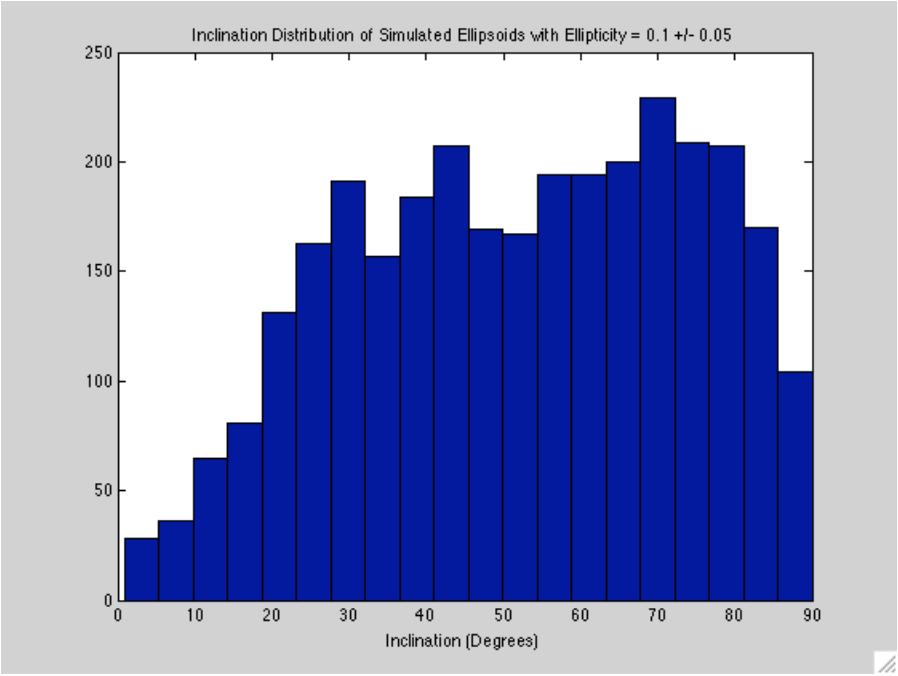

Figure 30: Inclinations of Simulated Galaxies with Ellipticity 0.10

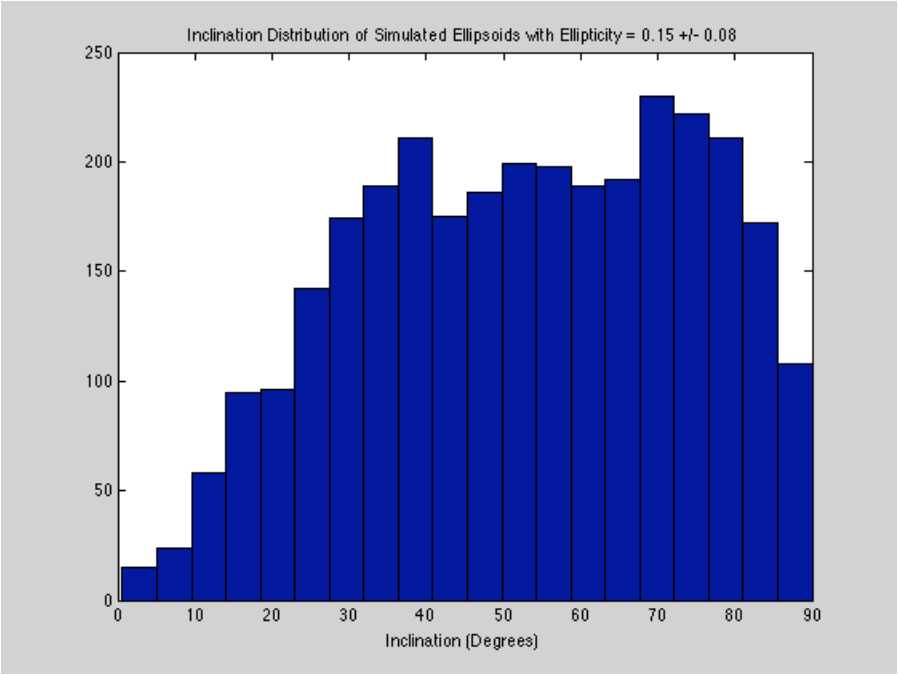

Figure 31: Inclinations of Simulated Galaxies with Ellipticity 0.15

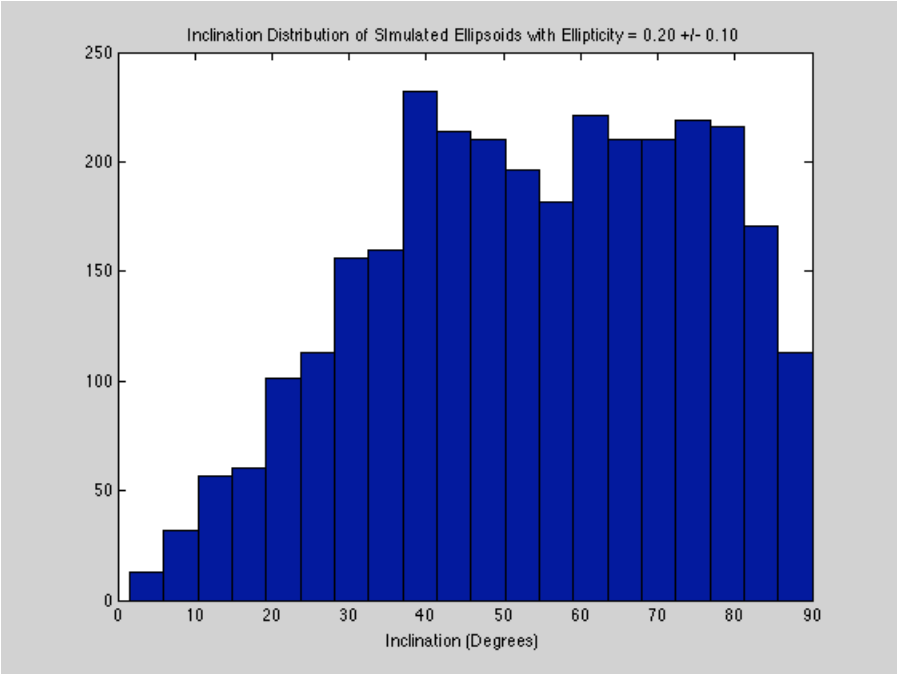

Figure 32: Inclinations of Simulated Galaxies with Ellipticity 0.20

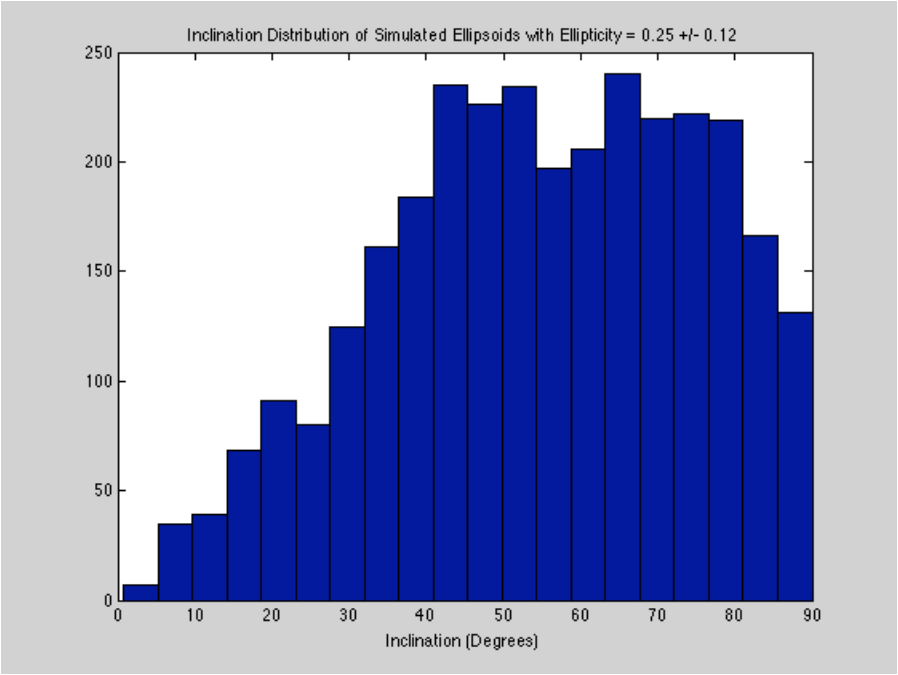

Figure 33: Inclinations of Simulated Galaxies with Ellipticity 0.25